SPi | Journal Code: G R L | Article ID: 5 3 3 1 1 | Dispatch: 19.08.15 | CE: MTM | No. of Pages: 8 | ME:

AGU PUBLICATIONS

Geophysical Research Letters

RESEARCH LETTER
10.1002/2015GL065665

Key Points:
- The climate system has a huge memory that can be exploited by scaling models
- Fractional Gaussian noise is adequate model for macroweather (10 days–30 years)
- Twentieth century hindcasts (including pause) are accurate with two parameters

Correspondence to:
S. Lovejoy,
lovejoy@physics.mcgill.ca

Citation:
Lovejoy, S. (2015), Using scaling for macroweather forecasting including the pause, *Geophys. Res. Lett.*, *42*, doi:10.1002/2015GL065665.

Received 3 AUG 2015
Accepted 5 AUG 2015
Accepted article online 7 AUG 2015

Using scaling for macroweather forecasting including the pause

S. Lovejoy[1]

[1]Physics Department, McGill University, Montreal, Quebec, Canada

Abstract The ScaLIng Macroweather model (SLIMM) is a new class of stochastic atmospheric model. It exploits the large system memory to overcome the biases of conventional numerical climate models, it makes hindcasts and forecasts over macroweather forecast horizons (≈10 days to decades). Using the simplest (scalar), SLIMM model with only two parameters, we present various twentieth century hindcasts including several of the slowdown ("pause") in the warming since 1998. The 1999–2013 hindcast is accurate to within ±0.11 K, with all the 2002–2013 anomalies hindcast to within ±0.02 K. In comparison, the Climate Model Intercomparison Project Phase 3 hindcasts were on average about 0.2 K too warm.

1. Introduction

Numerical climate models (coupled general circulation models: GCMs) are essentially weather models that are pushed far beyond their deterministic predictability limits (of the order 10 days): the weather they generate has no relation with the real weather, it is a "noise" forcing the lower frequencies. In this low-frequency "macroweather" regime, control runs—with fixed climate forcings (boundary conditions)—converge slowly to the GCM climates [*Lovejoy et al.,* 2013a]. However, due to model "biases," neither the statistics of the driving noise (the weather) nor the model climates are fully realistic.

Following *Hasselmann* [1976], alternative stochastic models have been developed, the most sophisticated of which are the Linear Inverse Models (LIM), [*Penland*, 1996; *Penland and Sardeshmuhk*, 1995], [*Newman et al.,* 2003], [*Sardeshmukh et al.,* 2000], [*Sardeshmukh and Sura*, 2009]. In principle, stochastic models have the advantage that their statistics can be made realistic; and by exploiting empirical data (the system "memory"), they can effectively be forced to converge to the real climate so that, for example, a 20 component implementation of the LIM model (with >100 parameters) can already do somewhat better than GCMs for global annual temperature forecasts [*Newman*, 2013].

The key question for stochastic macroweather models is thus how big is the system memory and how best to exploit it? The LIM approach is based on systems of coupled ordinary (integer ordered) differential equations whose solutions are essentially white noises and their integrals (Ornstein-Uhlenbeck processes). Their low-frequency limits are (unpredictable) white noises so that for horizons beyond about 2 years, the errors rapidly increase [*Newman*, 2013]. However, over the last decades, a scaling paradigm for atmospheric variability has evolved that implies the existence long-range—potentially huge—memories, and these can be exploited for forecasting [*Lovejoy and Schertzer*, 1986; *Pelletier*, 1998; *Koscielny-Bunde et al.,* 1998; *Franzke,* 2010, 2012; *Rypdal et al.,* 2013; *Rypdal and Rypdal*, 2014; *Yuan et al.,* 2014; *Lovejoy*, 2014c] (see the reviews of *Lovejoy and Schertzer* [2010], *Lovejoy and Schertzer* [2012], and *Lovejoy and Schertzer* [2013]).

In a recent paper, we show how to use the simplest relevant scaling model—fractional Gaussian noise—to exploit the system memory: the ScaLIng Macroweather Model (SLIMM) [*Lovejoy et al.,* 2015] (hereafter LDH). SLIMM was shown to make skilful hindcasts of natural variability from monthly to decadal scales (LDH). The key to overcoming the limitations of an earlier attempt to exploit the scaling [*Baillie and Chung*, 2002] was to use the empirical effective climate sensitivity ($\lambda_{2\times CO_2}$) to remove the anthropogenic effects [*Lovejoy*, 2014b]. For annually, globally averaged temperatures, the resulting two parameter SLIMM model ($\lambda_{2\times CO_2}$ and the scaling exponent H, see below) was already generally better than both initialized GCMs and LIM, although LIM was marginally better for horizons up to about 2 years (LDH). In this paper, we demonstrate SLIMM on hindcasts and forecasts, notably showing that the slowdown in the warming since 1998—the pause is well hindcast as a natural cooling event immediately following a massive prepause

warming event (1992–1998). The present results can be viewed as the conditional probability extensions of a recent unconditional (return period) analysis [*Lovejoy*, 2014a].

2. Methods

In the weather regime, atmospheric dynamics are intermittent; the corresponding stochastic models are highly nonlinear, they are based on multiplicative cascade processes (see *Lovejoy and Schertzer* [2013], Chapter 5 for a review). However, in the macroweather regime, the intermittency is much weaker so that as a first approximation, nonintermittent (quasi-Gaussian) models may be used (although not for the extremes, see below). The usual starting point (e.g., for LIM) is the ordinary differential equation:

$$\left(\frac{d}{dt}+\omega_w\right)T(t)=\sigma_\gamma\gamma(t) \tag{1}$$

where $\omega_w=\tau_w^{-1}$ is the "weather frequency," σ_γ is the amplitude of the forcing, and $\gamma(t)$ is a Gaussian white noise forcing with mean $<\gamma(t)>=0$. By putting $d/dt\approx 0$, we see that in the low-frequency limit, $T(t)$ is a white noise. The key to realistic modeling of frequencies lower than ω_w is therefore to use a (low frequency) fractional order generalization:

$$\frac{d^{H+1/2}T}{dt^{H+1/2}}=\sigma_\gamma\gamma(t)\leftrightarrow \quad T(t)=\frac{\sigma_\gamma}{\Gamma(H+1/2)}\int_{-\infty}^{t}(t-t')^{-(1/2-H)}\gamma(t')dt';\ -1/2<H<0 \tag{2}$$

where the right-hand side is the solution obtained by (Riemann-Liouville) fractional integration of both sides of the equation by order $H+1/2$, Γ is the usual gamma function. Equation (2) defines the simplest (scalar) SLIMM model; the low-frequency part of the LIM paradigm is recovered as the special case with $H=-1/2$.

The solution $T(t)$ is a (stationary) "fractional Gaussian noise" process. At small scales, it has singular behavior so that the temporal resolution τ of $T(t)$ is fundamentally important. Although physically, the weather scales are responsible for the smoothing at τ_w, in practice, we typically have macroweather data averaged at even lower resolutions: for example, monthly or annually. The simplest procedure is to introduce the resolution simply as an averaging procedure yielding $T_\tau(t)$ so that the variance $\langle T_\tau^2\rangle=\sigma_T^2\tau^{2H}$ diverges in the small resolution limit (LDH, recall $H<0$), it follows that the spectrum of T is $E(\omega)\approx\omega^{-\beta}$, ω is the frequency, and $\beta=1+2H$. To within an additive and multiplicative constant, the integral of $T(t)$ (denoted S below) is a fractional Brownian motion process introduced by *Kolmogorov* [1940] and *Mandelbrot and Van Ness* [1968]. In *Lovejoy and de Lima* [2015], we show how to extend this scalar SLIMM to spatially intermittent space-time SLIMM (accounting for different climatic regions).

A straightforward way of predicting the future $\hat{T}(t)(t>0)$ from past information ($T(t)$, $t\le 0$) is to use the method of innovations: we discretize equation (2), writing it as a matrix equation. The matrix is then inverted to yield the corresponding past "innovations" $\gamma(t)$ for $t\le 0$. To make the forecast at time $t>0$, equation (2) uses the past ($t\le 0$) values for $\gamma(t)$ but for $t>0$, it uses $\gamma(t)=<\gamma(t)>=0$. A variant, also illustrated below, is to replace the innovations for $t>0$ by independent Gaussian random variables, the results are future realizations (at times $t>0$) conditioned on the past (the values at $t\le 0$). As discussed in LDH, in future it may be advantageous to use other approaches by notably following *Gripenberg and Norros* [1996] (integral equations) discretized with a variant of the *Hirchoren and Arantes* [1998] method, which notably has the advantage of requiring less past data.

In LDH, the NASA Goddard Institute for Space Studies (GISS) temperature series were analyzed, the global-scale exponent was estimated as $H\approx -0.20\pm 0.03$ and the theoretical variance of forecast errors was derived. It was shown that with this H value, for forecasts of one nondimensional time (resolution) unit (e.g., a month, a year) in the future, 35% of the error variance can be explained by the forecast (over oceans, $H\approx -0.1$ and $\approx 65\%$ can be explained; note that we found subsequently that other global series tended to have Hs that were a little closer to -0.1 than -0.2). Hindcasts from 1900 to 2003 confirmed the theoretical error and correlation estimates and showed that the RMS error for 1 year globally, annually averaged hindcasts was ±0.093 K compared to the range ±0.105 to ±0.11 K for initialized GCMs and ±0.085 K for the LIM model (Table 2 in LDH). See also *Rypdal and Rypdal* [2014] for a supporting discussion of scaling versus (nonscaling) ~~First Assessment Report~~ processes.

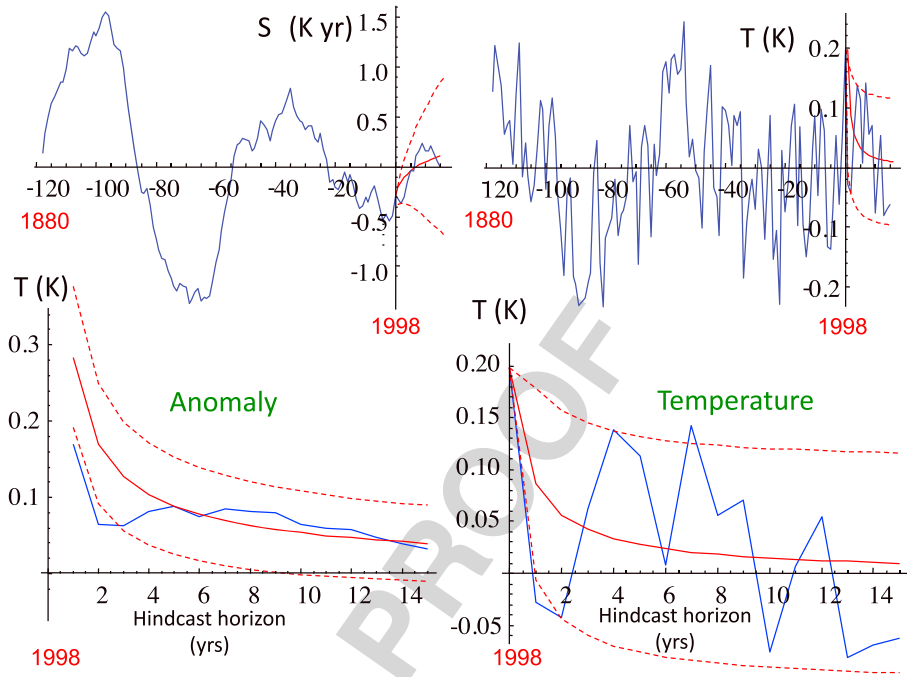

Figure 1. (top left) The summed (natural) global, annual temperature $S(t)$ (blue) with the hindcast (red) from 1998 shown in red (here and elsewhere, the dashed red lines are 1 standard deviation error limits). (top right) The natural temperature (blue) with the hindcast from 1998 (red). (bottom left) The anomaly defined as the average natural temperature (i.e., residue) over the hindcast horizon (blue), red is the hindcast. (bottom right) The temperature since 1998 (blue) with hindcast (red), a blowup of the hindcast part of Figure 1 (top right).

3. Results

To illustrate the method, we used the NASA GISS annually, globally averaged series from 1880 through 2013. The first step was to estimate the natural variability by regressing the temperature against the CO_2 radiative forcing (using $\lambda_{2\times CO_2} = 2.33 \pm 0.16$ K/CO_2 doubling) and taking the residues. If one prefers, one can use the estimated equivalent CO_2 (CO_2eq), but this involves extra assumptions (including on aerosols) and leads to sensitivities a factor 1.12 times smaller. However, since $\log_2 CO_2$ and $\log_2 CO_2$eq are highly correlated ($r^2 = 0.993$), the residues are virtually identical. Unlike initialized GCM hindcasts that "optimistically" assume that future solar and volcanic forcings are known, our hindcasts (statistically) take these into account. The resulting residues (shown in the upper right curve in Figure 1) F1 have RMS variations of ±0.109 K that are very close to the GCM errors mentioned above as well as to the variance of preindustrial multiproxies; the residues must be very close to the true natural variability. This annual resolution zero-lagged forcing-response relation is only the simplest: introducing a time lag or power law Green's function (transfer function) may be physically more realistic but makes very little difference to the amplitudes of the residues and—in any event, as shown in LDH—the zero-lagged residues have well-defined scaling properties that allow them to be forecast with skill that approaches the theoretical maximum.

In Figure 1, we compare the annual temperature residues (T) and its running sum $s(t) = \sum_{t' \le t} T(t')$ with their SLIMM hindcasts (red) and theoretical 1 standard deviation error bars (dashed). As expected, the actual temperatures are seen to lie almost entirely within the limits. Figure 1 (bottom right) shows a blowup of the temperature hindcast and the actual temperature residues, and Figure 2a shows the difference (error); F2 we see that over the entire period 1998–2013, the maximum forecast error is ≈ ±0.11 K. However, the error for the hindcast "anomalies" is considerably smaller (i.e., the residues averaged over the hindcast horizon t: $(\hat{S}(t) - S(0))/t$): Figure 1 (bottom left) and Figure 2a (blue). Beyond 2 years, the anomalies are within the theoretical 1 standard deviation limits, from 2002 to 2013, the anomaly errors are ≤ ±0.02 K, i.e., below the

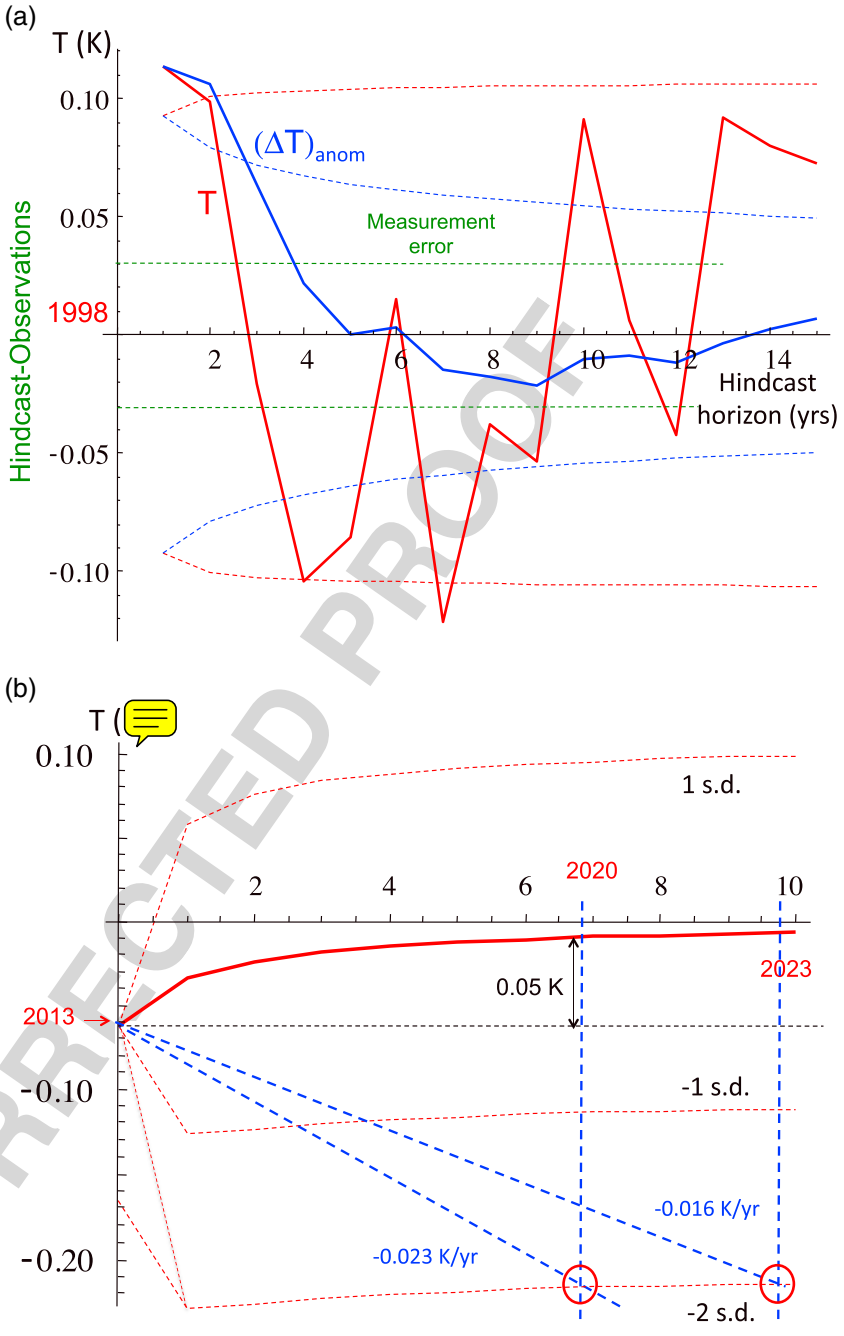

Figure 2. (a) The hindcast errors: anomalies (blue) and temperatures (red) obtained from Figure 3 (bottom left and right, respectively). The 1 standard deviation error limits are shown as dashed. The largest absolute errors are ±0.11 K. Also shown is the estimate of the accuracy of the observations (dashed green), about ±0.03 K. (b) The future natural temperature as forecast using the past temperature data to 2013 and exponent $H = -0.2$. We see that the temperature is forecast to return to the long-term trend (zero) fairly quickly. Also shown are the +1, −1, and −2 standard deviation limits. The dashed blue lines show the natural cooling trends needed to offset projected anthropogenic warmings of 0.023 K/yr and 0.016 K/yr (corresponding to $d\log_2 CO_2/dt = 0.01$/year and 0.007/year, respectively). These allow us to estimate how long the pause can last without invalidating the anthropogenic warming hypothesis (red circles and vertical lines).

estimated temperatures measurement errors (±0.03 K) [*Lovejoy et al.,* 2013b]. (The term "anomaly" is a short hand for the anomaly fluctuation, for the residues this is simply the series at a specific resolution. For example, the RMS accuracy of annual GCM hindcasts is often quoted after averaging them over 4 or 5 years, this is the RMS of the 4 or 5 year anomaly). We could mention that other "mean reverting" processes such as LIM will

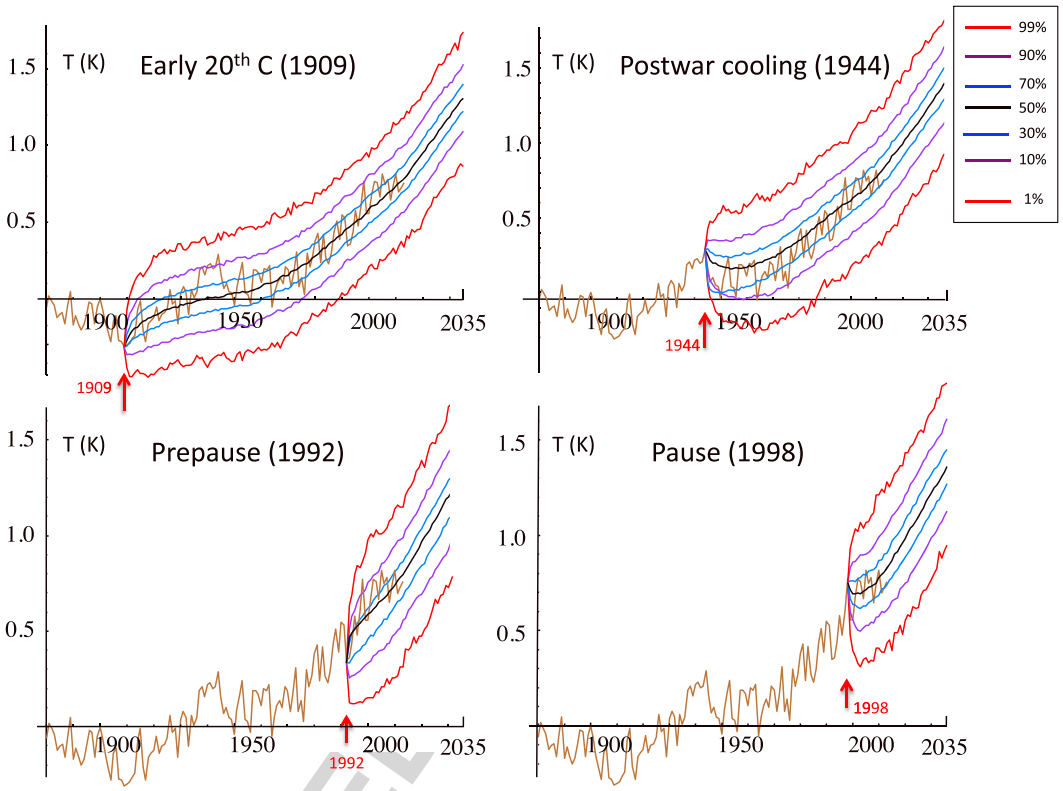

Figure 3. Hindcasts starting in 1909, 1944, 1992, and 1998 each using the exponent $H = -0.2$, the effective climate sensitivity (zero lag) of 2.33 K/CO_2 doubling, the prior temperature data back to 1880 as well as the actual global annual averaged CO_2 concentration from *Frank et al.* [2010], extended to 2013 as described in [*Lovejoy*, 2014a]. The brown lines are the actual (NASA GISS) annual global temperature series, and the colored lines are for the percentiles as indicated. The curves beyond 2013 are forecasts based on $\log_2 CO_2$ concentrations projected to increase by 0.01/year. In 2035, this yields 460 ppm which is a little higher than Representative Concentration Pathway 4.5 (RCP 4.5) (450 ppm) but lower than RCP 8.5 (470 ppm). The extrapolation uses the same effective climate sensitivity implying a 0.58 K increase from 2010 to 2035 which is about the mean of the AR4 SRES scenarios (see Figure 4).

also show qualitatively the same behavior: the superiority of SLIMM was quantitatively established in LDH using over 100 hindcasts from 1900 to 2003.

Since it can be so accurately hindcast, these results support the (unconditional) statistical analysis of *Lovejoy* [2014a] that the pause must be due to natural variability. This is consistent with *Steinman et al.* [2015] who singled out particular high-amplitude—but narrow-scale range—low-frequency natural processes including the Atlantic Multidecadal Oscillation (AMO) and argued that they explain the pause. However, due to the scaling (in space and in time) there is in fact a hierarchy of processes analogous to the AMO [*Held et al.,* 2010]: our hindcasts statistically account for the whole relevant scale range and show that they are all important.

While this paper was under review, an improved temperature series appeared [*Karl et al.,* 2015] displaying a weaker "pause." Whereas in the series analyzed here, it was strong enough to recur on average only every 20–50 years [*Lovejoy*, 2014a], in the new series this return period was reduced to only about 10 years [*Lovejoy*, 2015] so that decadal trends were not statistically significant.

We can SLIMM to make a decadal temperature forecast (2014–2023), Figure 2b. We see that the forecast is for a gradual return to the long-term trend (i.e., to zero for the residues, to the anthropogenic warming trend for the actual temperatures). To forecast the total temperature change (natural plus anthropogenic), we used projected increases of $d\log_2 CO_2/dt = 0.01$/year and ≈ 0.007/year (corresponding to warming trends of 0.023 K/yr and 0.016 K/yr) that are, respectively, $\approx 40\%$ larger than and equal to the trend since 2000; the former gives projections close to the International Panel on Climate Change (IPCC) Fourth Assessment

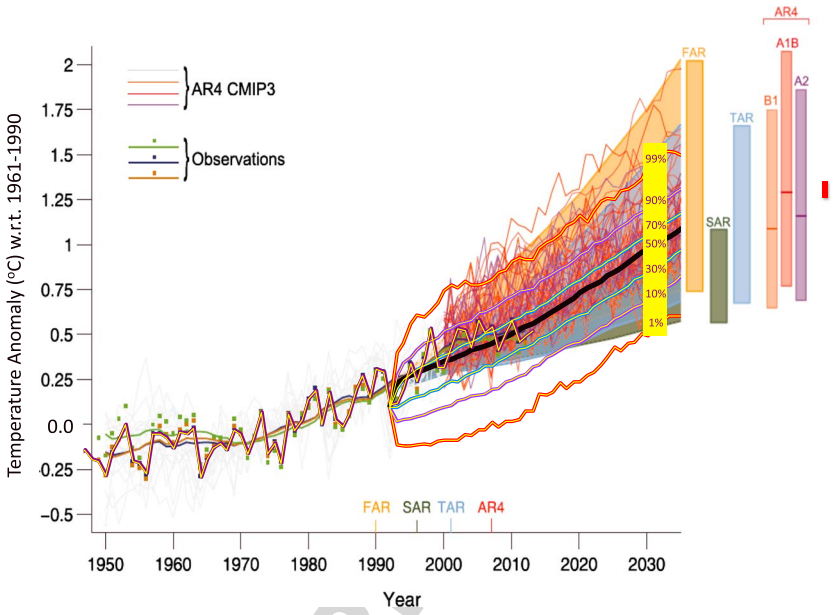

Figure 4. Using the method in Figure 3, this compares SLIMM hindcasts from 1992 with the individual CMIP3 runs "harmonized" to start from the same value in 1990 (adapted from Figure 1.4 AR5) and observations (the striped brown-yellow line is the NASA GISS series used above). The forecast to 2035 is based on the projected CO_2 and effective climate sensitivity as in Figure 2b. The black line is the hindcast/forecast mean, the striped thick lines indicate the percentile values indicated in the yellow rectangle. While the scaling hindcast is in good agreement, the maximum error—in 1998—is <0.2 K; in comparison, the swarm of individual GCM forecasts was generally a bit too high, with the mean near the 90% mark for the SLIMM hindcast (from ≈ 2000, too warm by ≈ 0.2 K).

Report (AR4) SRES scenarios discussed below. With these projections, the forecast for 2023 is for an increase Q6
of 0.28 ± 0.11 K, 0.21 ± 0.11 K above 2013 (the errors come from the predicted SLIMM forecast error and the uncertainty in $\lambda_{2\times CO_2}$). Even if the CO_2 concentrations stay in the lower range, the higher-warming value is relevant if the somewhat larger 20 year lagged $\lambda_{2\times CO_2}$ is used (see the discussion in *Lovejoy* [2014a]). The figure also shows the $+1$, -1, and -2 standard deviation limits. These allow us to estimate how long the pause can last without invalidating the anthropogenic warming hypothesis. From the graph, we see that if natural coolings continue until about 2020 and 2023 (respectively, for $d\log_2 CO_2/dt = 0.01$/year and ≈ 0.007/year, the dashed vertical lines), they would be 2 standard deviations below the forecast mean (solid red). This implies that—depending on the emissions and future concentrations—if the temperature in, respectively, 2020 or 2023 is the same as in 2013, the anthropogenic warming hypothesis may be rejected with 97.5% confidence.

We can now compare the full hindcast (natural plus anthropogenic) with the data. Figure 3 shows the result F3
for four different starting dates (1909, 1944, 1992, and 1998), along with confidence estimates indicated by various percentiles. Whereas the hindcasts shown in the previous figures were for the theoretical minimum square hindcast (equivalent here to the expectation conditioned on the observations), the hindcasts and percentiles below were each determined from 1000 stochastic simulations conditioned on the past observations as described above using only two parameters: $\lambda_{2\times CO2}$ and H. To underline the versatility of the approach, the noise $\gamma(t)$ was not assumed to be Gaussian but rather a more extreme distribution with an asymptotic power law ("heavy") tail with exponent $q_D = 4$ (i.e., slightly heavier than the observations in *Lovejoy* [2014b] and calculated with the method given in the appendix of the latter). Since the distribution was nearly identical to the Gaussian over the percentile ranges ≈ 2.5–97.5%, only the red 1%, and 99% lines are more extreme than for Gaussians. The agreement is excellent and any biases due to the method of separating anthropogenic and natural variability are small. Also shown in Figure 3 are the projections from 2013 to 2035.

Finally, we can compare the hindcast (from 1992) and projection with those made by GCMs (Figure 4). F4
Although for the AR4 simulations, the results of individual GCM outputs are shown, they appear as a "swarm," their mean is near the 90% SLIMM percentile which is about 0.2 K above the empirical mean temperature

(see e.g., *Guemas et al.* [2013], *Schmidt et al.* [2014], and *Steinman et al.* [2015] for discussion and theories). In contrast, the SLIMM hindcast avoids these biases and stays very close to the data.

4. Conclusions

Numerical climate models are biased both because the statistics of their random weather forcings and the GCM climates are not fully realistic. Stochastic models can improve on this by using empirically based statistics for the noise and by exploiting the system memory to force forecasts to converge to the real climate. Existing stochastic models (e.g., LIM) assume that there is only a short-term (exponentially damped) memory and show little skill beyond 2–3 years. In contrast, it has become increasingly clear that the atmosphere and climate system have a long-range memory and this can be exploited in scaling models. In this paper, we give examples using the simplest such model, the ScaLIng Macroweather Model (SLIMM), that is based on fractional Gaussian noise. Although in its simplest (scalar, single time series) form discussed here, it has only two parameters (one to remove the anthropogenic effects, the other an exponent quantifying the memory of the residuals), SLIMM already makes annual global hindcasts that are somewhat more accurate than initialized GCMs and displays skill up to decadal scales. Here I illustrated this on twentieth century hindcasts (from 1909, 1944, 1992, and 1998) as well as with a decadal forecast. I notably found that the pause in the warming (from 1998) is well hindcast with predicted annual temperatures errors $< \pm 0.11$ K (1999–2013) and with anomalies from 2002 to 2013 having errors $\leq \pm 0.02$ K. In comparison, the Coupled Model Intercomparison Project Phase 3 (CMIP3) hindcasts discussed in the IPCCs AR5 are on average about 0.2 K too high. These results are consistent with *Steinman et al.* [2015] but effectively extend them over a wide range of scales using the observed scaling statistics.

In future publications, we investigate space-time extensions of SLIMM and make regional monthly to decadal scale forecasts.

Acknowledgments
This work was unfunded, and there were no conflicts of interest. We thank L. del Rio Amador, R. Hébert, and D. Clarke for useful discussions. We also thank referees M. Crucifix and M. Rypdal for helpful critiques. The global annual temperature data are from the NASA GISS site.

The Editor thanks Michael Crucifix and an anonymous reviewer for their assistance in evaluating this paper.

References

Baillie, R. T., and S.-K. Chung (2002), Modeling and forecasting from trend-stationary long memory models with applications to climatology, *Int. J. Forecast.*, *18*, 215–226.
Frank, D. C., J. Esper, C. C. Raible, U. Buntgen, V. Trouet, B. Stocker, and F. Joos (2010), Ensemble reconstruction constraints on the global carbon cycle sensitivity to climate, *Nature*, *463*(28), doi:10.1038/nature08769.
Franzke, C. (2010), Long-range dependence and climate noise characteristics of Antarctica temperature data, *J. Clim.*, *23*, 6074–6081, doi:10.1175/2010JCL13654.1.
Franzke, C. (2012), Nonlinear trends, long-range dependence and climate noise properties of temperature, *J. Clim.*, *25*, 4172–4183, doi:10.1175/JCLI-D-11-00293.1.
Gripenberg, G., and I. Norros (1996), On the prediction of fractional Brownian motion, *J. Appl. Prob.*, *33*, 400–410.
Guemas, V., F. J. Doblas-Reyes, I. Andreu-Burillo, and M. Asif (2013), Retrospective prediction of the global warming slowdown in the past decade, *Nat. Clim. Change*, *3*, 649–653.
Hasselmann, K. (1976), Stochastic climate models, part I: Theory, *Tellus*, *28*, 473–485.
Held, I. M., M. Winton, K. Takahashi, T. Delworth, F. Zeng, and G. K. Vallis (2010), Probing the fast and slow components of global warming by returning abruptly to preindustrial forcing, *J. Clim.*, *23*, 2418–2427.
Hirchoren, G. A., and D. S. Arantes (1998), Predictors for the discrete time fractional Gaussian processes, in *Telecommunications Symposium, 1998. ITS '98 Proceedings. SBT/IEEE International*, pp. p49–p53, IEEE, Sao Paulo.
Karl, T. R., A. Arguez, B. Huang, J. H. Lawrimore, J. R. McMahon, M. J. Menne, T. C. Peterson, R. S. Vose, and H.-M. Zhang (2015), Possible artifacts of data biases in the recent global surface warming hiatus, *Sci. Express*, *348*, 1469–1472, doi:10.1126/science.aaa5632.
Kolmogorov, A. N. (1940), Wienershe spiralen und einige andere interessante kurven in Hilbertschen Raum, *Dokl. Acad. Nauk S.S.S.R.*, *26*, 115–118.
Koscielny-Bunde, E., A. Bunde, S. Havlin, H. E. Roman, Y. Goldreich, and H. J. Schellnhuber (1998), Indication of a universal persistence law governing atmospheric variability, *Phys. Rev. Lett.*, *81*, 729–732.
Lovejoy, S. (2014a), Return periods of global climate fluctuations and the pause, *Geophys. Res. Lett.*, *41*, 4704–4710, doi:10.1002/2014GL060478.
Lovejoy, S. (2014b), Scaling fluctuation analysis and statistical hypothesis testing of anthropogenic warming, *Clim. Dyn.*, *42*, 2339–2351, doi:10.1007/s00382-014-2128-2.
Lovejoy, S. (2014c), A voyage through scales, a missing quadrillion and why the climate is not what you expect, *Clim. Dyn.*, doi:10.1007/s00382-014-2324-0.
Lovejoy, S. (2015), Climate closure, *EOS* in press.
Lovejoy, S., and D. Schertzer (1986), Scale invariance in climatological temperatures and the local spectral plateau, *Ann. Geophys.*, *4B*, 401–410.
Lovejoy, S., and D. Schertzer (2010), Towards a new synthesis for atmospheric dynamics: Space-time cascades, *Atmos. Res.*, *96*, 1–52, doi:10.1016/j.atmosres.2010.01.004.
Lovejoy, S., and D. Schertzer (2012), Low frequency weather and the emergence of the climate, in *Extreme Events and Natural Hazards: The Complexity Perspective*, edited by A. S. Sharma et al., pp. 231–254 , AGU monographs, Washington, D. C.
Lovejoy, S., and D. Schertzer (2013), *The Weather and Climate: Emergent Laws and Multifractal Cascades*, 496, Cambridge Univ. Press, Cambridge, U. K.

Lovejoy, S., and M. I. P. de Lima (2015), The joint space-time statistics of macroweather precipitation, space-time statistical factorization and macroweather models, *Chaos*, *25*, 075410, doi:10.1063/1.4927223.
Lovejoy, S., D. Schertzer, and D. Varon (2013a), Do GCMs predict the climate…. or macroweather?, *Earth Syst. Dyn.*, *4*, 1–16, doi:10.5194/esd-4-1-2013.
Lovejoy, S., D. Scherter, and D. Varon (2013b), How scaling fluctuation analyses change our view of the climate and its models (Reply to R. Pielke sr.: Interactive comment on "Do GCMs predict the climate… or macroweather?" by S. Lovejoy et al.), *Earth Syst. Dyn. Discuss.*, *3*, C1–C12.
Lovejoy, S., L. del Rio Amador, and R. Hébert (2015), The Scaling LInear Macroweather model (SLIM): Using scaling to forecast global scale macroweather from months to decades, *Earth System Dyn. Discuss*, *6*, 489–545, doi:10.5194/esdd-6-489-2015.
Mandelbrot, B. B., and J. W. Van Ness (1968), Fractional Brownian motions, fractional noises and applications, *SIAM Rev.*, *10*, 422–450.
Newman, M. (2013), An empirical benchmark for decadal forecasts of global surface temperature anomalies, *J. Clim.*, *26*, 5260–5269, doi:10.1175/JCLI-D-12-00590.1.
Newman, M. P., P. D. Sardeshmukh, and J. S. Whitaker (2003), A study of subseasonal predictability, *Mon. Weather Rev.*, *131*, 1715–1732.
Pelletier, J. D. (1998), The power spectral density of atmospheric temperature from scales of 10**-2 to 10**6 yr, *Earth Planet. Sci. Lett.*, *158*, 157–164.
Penland, C. (1996), A stochastic model of IndoPacific sea surface temperature anomalies, *Phys. D*, *98*, 534–558.
Penland, C., and P. D. Sardeshmuhk (1995), The optimal growth of tropical sea surface temperature anomalies, *J. Clim.*, *8*, 1999–2024.
Rypdal, K., L. Østvand, and M. Rypdal (2013), Long-range memory in Earth's surface temperature on time scales from months to centuries, *J. Geophys. Res. Atmos.*, *118*, 7046–7062, doi:10.1002/jgrd.50399.
Rypdal, M., and K. Rypdal (2014), Long-memory effects in linear response models of Earth's temperature and implications for future global warming, *J. Clim.*, *27*(14), 5240–5258, doi:10.1175/JCLI-D-13-00296.1.
Sardeshmukh, P. D., and P. Sura (2009), Reconciling non-Gaussian climate statistics with linear dynamics, *J. Clim.*, *22*, 1193–1207.
Sardeshmukh, P., G. P. Compo, and C. Penland (2000), Changes in probability associated with El Nino, *J. Clim.*, *13*, 4268–4286.
Schmidt, G. A., D. T. Shindell, and K. Tsigaridis (2014), Reconciling warming trends, *Nat. GeoSci.*, *7*, 158–160.
Steinman, B. A., M. E. Mann, and S. K. Miller (2015), Atlantic and Pacific multidecadal oscillations and Northern Hemisphere temperatures, *Science*, *347*, 988–991, doi:10.1126/science.1257856.
Yuan, N., Z. Fu, and S. Liu (2014), Extracting climate memory using fractional integrated statistical model: A new perspective on climate prediction, *Sci. Rep.*, *4*, 6577, doi:10.1038/srep06577.